# Cyclic Multi-directional Response of Clay Deposits: Evaluating a Constitutive Model

**Nouri H. Author, Ph.D., P.E., M.ASCE[1] Rutherford C. Author, Ph.D., P.E., M.ASCE[2] and Biscontin G. Author, Ph.D., M.ASCE[3]**

[1] Shannon and Wilson Inc., 400 North 34th Street Suit 100, P.O. Box 300303, Seattle, WA 98103; e-mail: Nouri.hreza@gmail.com; hrn@shanwil.com
[2] Department of Civil, Construction and Environmental Engineering (CCEE), Iowa State University, 406 Town Engr Ames, IA 50011; e-mail: cassier@iastate.edu
[3] Department of Engineering, University of Cambridge, Schofield Centre High Cross, Madingley Road, Cambridge, United Kingdom CB3 0EL; e-mail: gb479@cam.ac.uk

## ABSTRACT

The focus of this study is to verify the capabilities of a constitutive model to mimic a wide range of monotonic and cyclic multi-directional stress paths in clays. The generalized elasto-plastic constitutive formulation of the model enables to describe stress-strain response, accumulation of permanent deformations and excess pore pressure in monotonic and multi-directional cyclic loading. The model is calibrated based on the experimental database on the Gulf of Mexico clay developed at Texas A&M, including the constant rate strain (CRS) consolidation as well as monotonic triaxial tests. Capabilities of the calibrated model to predict the cyclic multi-directional stress paths are then evaluated through comparison with the results of cyclic, circular, and figure 8 multi-directional simple shear tests as a part of the Gulf of Mexico clay experimental database. We also used the extensive database for Boston Blue Clay (BBC) to calibrate model constants and verify its capabilities to mimic the monotonic and cyclic response of lower plasticity clays. The model proves successful to predict a wide range of complicated cyclic multi-directional stress paths for clays.

## INTRODUCTION

The paradigm of geotechnical analysis and design is shifting from the conventional “safety factor” design to performance based engineering to achieve a safe yet sustainable and economical design. Reasonable prediction of the performance (i.e. deformation) of geotechnical structures under complicated extreme loading conditions calls for powerful numerical tools and predictive yet simple constitutive formulations, calibrated and verified through element tests, physical models, and case histories. Application of comprehensive constitutive models to simulate liquefaction in saturated coarse grain material is becoming a state of geotechnical

engineering practice through the implementation and application of UBCSAND (Beaty and Byrne 2011) and PM4SAND (Ziotopoulou and Boulanger 2013) in numerical simulation of geotechnical boundary value problems. However, the geotechnical engineering practice lacks a constitutive equation to realistically mimic the cyclic response of clays and reasonably predict the consequences including strain softening. Besides, the multi-directional nature of the earthquake loads is often overlooked in the performance-based analysis and deformation prediction of the geotechnical structures due to its complexity and poor understanding of the behavioral and modeling aspects of the problem. To this end, Nouri (2013) developed a constitutive model to predict the monotonic and cyclic response of clays. Nouri (2013) verified the predicting capabilities of the model for a wide range of stress paths for different clays including Boston Blue Clay (BBC), Lower Cromer Till (LCT), San Francisco Bay Mud (SFBM), and Gulf of Mexico Clay (GMC). The focus of this paper is to present a modified formulation which captures the strain rate effect as a key factor to mimic cyclic response of clays. The proposed constitutive equation is calibrated and verified for a low and high plasticity clay (i.e. BBC and GMC respectively) and the predictive capabilities of the model to reasonably mimic the complicated cyclic mono and multidirectional stress paths are demonstrated.

## OVERVIEW OF THE CONSTITUTIVE MODEL

The basis of our constitutive formulation is the SANICLAY (Simple ANIsotropic CLAY) model proposed by Dafalias et al. (2006). We selected SANICLAY due to its minimal number of parameters, reasonable accuracy in the predictions, and its modular setup which lends itself to further modifications. Built on the premises of the critical state soil mechanics, SANICLAY is the generalized form of the Modified Cam Clay (MCC) to account for the inherent and evolving anisotropy. SANICLAY is a rate-independent model which is performing well in predicting the response of normally consolidated (NC) clay but does not generate plastic deformations and excess pore pressure during cyclic loading. Given the objectives of the current study to predict cyclic behavior, we implemented some modifications in the formulation, mainly by:

- using the lemniscate bounding surface plasticity instead of elliptical yield surface in SANICLAY (Fig. 1) to better capture the undrained shear strength of over-consolidated (OC) clays and develop plastic strain and excess pore pressure within bounding surface.
- applying the non-linear elasticity formulation instead of the MCC based isotropic linear elastic equation in SANICLAY model.
- incorporating the strain rate effect as a key factor for enhanced prediction of stress-strain-strength behavior of NC clay during cyclic or higher rate loading.

**Flow rule.** Flow rule in our model is non-associated [i.e. yield surface ($f$) different than the plastic potential ($g$)]. Similar to SANICLAY, plastic potential is a distorted and disoriented elliptical surface (Fig. 1) to account for the effect of initial anisotropy, which is basically used to obtain the amount and direction of the plastic deformation. Eq. 1 shows the equations for plastic

potential surface in triaxial and multi-axial stress spaces. Note that the triaxial mean and deviatoric effective stresses are $p=(\sigma_{yy}+2\sigma_{xx})/3$ and $q=\sigma_{yy}-\sigma_{xx}$, while in multi-axial space $p=(\sigma_{xx}+\sigma_{yy}+\sigma_{zz})/3$ and $q=\sqrt{1.5\mathbf{S}:\mathbf{S}}$ where $\mathbf{S}=\boldsymbol{\sigma}-p\mathbf{I}$ denotes tensorial deviatoric stress:

$$\begin{aligned} &g=(q-p\alpha)^2-(M^2-\alpha^2)p(p_a-p)=0 && \text{Triaxial}\\ &g=\frac{3}{2}(\mathbf{S}-p\boldsymbol{\alpha}):(\mathbf{S}-p\boldsymbol{\alpha})-(M^2-\frac{3}{2}\boldsymbol{\alpha}:\boldsymbol{\alpha})p(p_a-p)=0 && \text{Multi-axial}\end{aligned} \tag{1}$$

$\alpha$ defines the inherent anisotropy and appears as a scalar-valued slope in the triaxial ($q$-$p$) space (Fig. 1) and as a tensor ($\boldsymbol{\alpha}$) in multi-axial space. The evolving anisotropy is also defined by the evolution of $\alpha$, i.e. the rotation of $\alpha$ line and plastic potential. $p_a$ denotes the size of plastic potential and corresponds to the value of $p$ at $q=p\alpha$ (Fig. 1). $M$ is the slope of the critical state line in deviatoric/mean effective stress space (the critical state ratio) based on the Mohr-Coulomb failure criterion and equals to critical state ratio in compression ($M_c$) for $\eta>\alpha$ and critical state ratio in extension ($M_e$) for $\eta<\alpha$.

**Yield surface.** To better capture the undrained response of OC clays, we adopted the anisotropic lemniscate as the yield surface after some modifications in the original formulation introduced by Pestana (1994). Fig. 2 compares the isotropic and anisotropic shapes of the SANICLAY elliptical yield surface with the lemniscate, which shows the increased difference in the shapes in the dry or supercritical region in compression regime. The formulation in the triaxial and multi-axial stress spaces is as below:

$$\begin{aligned} &f=(q-p\beta)^2-\varsigma^2p^2\left(1-\left(\frac{p}{p_o}\right)^m\right)=0; && \varsigma^2=N^2+\beta^2-2\eta\beta && \text{Triaxial}\\ &f=\frac{3}{2}(\mathbf{S}-p\boldsymbol{\beta}):(\mathbf{S}-p\boldsymbol{\beta})-\varsigma^2p^2\left(1-\left(\frac{p}{p_o}\right)^m\right)=0; && \varsigma^2=N^2+\frac{3}{2}\boldsymbol{\beta}:\boldsymbol{\beta}-3\boldsymbol{\eta}:\boldsymbol{\beta} && \text{Multi-axial}\end{aligned} \tag{2}$$

The lemniscate yield surface is described with two model parameters of $N$ and $m$. Material parameter $N$ defines the slope of the lines tangential to the sides of the yield surface at the origin. This parameter controls the aperture of the surface (see Fig. 2). Parameter $m$ is used to characterize the shape of the curve; however for the sake of simplicity and also to keep the number of parameters minimal, $m$ is fixed as a constant equal to 0.5 in this study. $p_o$ quantifies the size of the yield surface and corresponds to the mean effective stress at stress ratio of $\eta=\beta$. Calibration of constant $N$ is done using the same procedure in SANICLAY, through the trial predictions for undrained triaxial compression response of the $K_o$-consolidated clay (*CKoUC*).

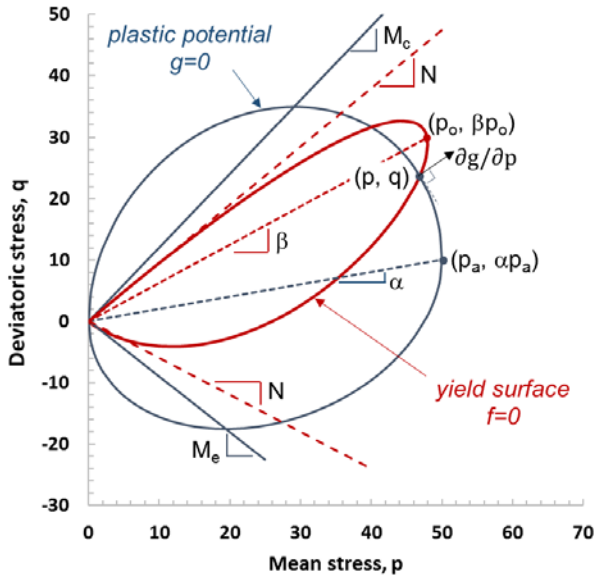


Figure 1- Lemniscate yield surface and plastic potential in triaxial stress space [reproduced from Dafalias et al. (2006)]

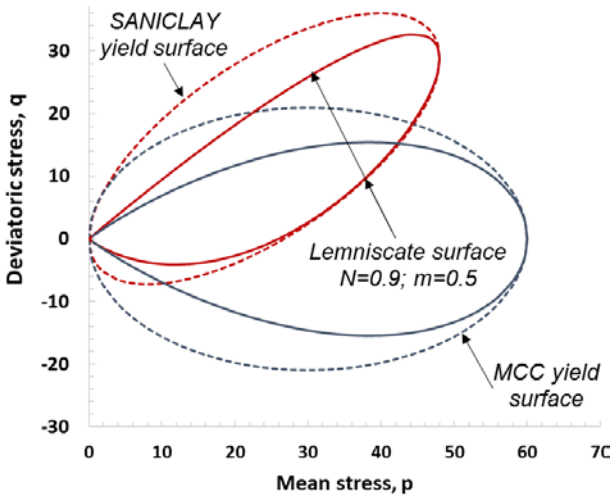


Figure 2- Comparison of isotropic and anisotropic elliptical yield surface with lemniscate (Pestana 1994)

**Non-linear elasticity.** The proposed constitutive model in this study uses the same methodology developed by Whittle and Kavadas (1994) in MIT-E3 model to formulate the non-linear elasticity and the perfect hysteretic loop. The loop is characterized by a piecewise continuous formulation with smoothly varying stiffness in between the two subsequent stress reversal points for unload-reload response of consolidation test using $\psi$ variable:

$$K = \frac{p(1+e_o)}{\kappa}; \qquad \kappa = \kappa_o(1+\delta); \qquad \delta = Dn(\ln\psi)^{n-1}; \qquad \psi = \max\left(\frac{p}{p_{rev}}, \frac{p_{rev}}{p}\right) \tag{3}$$

As shown in Fig. 3, $p_{rev}$ is the mean effective stress at the reversal point. $\kappa_o$ characterizes the small strain stiffness right after stress reversal point (i.e. $\psi$ =1, and $\delta$ =0) and therefore calibrated with the small strain stiffness or shear wave velocity. *D* and *n* are material parameters which describe the swelling response in one dimensional or isotropic consolidation test and could be calibrated by trial predictions to find the best fit for the unloading or swelling measured data (Fig. 3). Whittle and Kavadas (1994) generalized the formulation to account for effect of shear stresses to develop the hysteretic loop:

$$\delta = Dn(\ln\psi + \psi_s)^{n-1}; \qquad \psi_s = \sqrt{\left[\mathbf{w}(\mathbf{r}-\mathbf{r_{rev}}):\mathbf{w}(\mathbf{r}-\mathbf{r_{rev}})\right]} \tag{4}$$

$\psi_s$ is the measure of deviatoric distance of the current state from the most recent reversal state of stress. $\mathbf{r}$ and $\mathbf{r_{rev}}$ are stress ratios at the current and the last reversal stress points. Whittle

and Kavadas (1994) also introduced **w** tensor as an input parameter. The diagonal components are $w_{ii}$ =w and the off-diagonal components are equal to $w_{ij}$ =4w to better capture the simple shear response. This parameter basically controls the deviatoric non-linear behavior. w could be calibrated using the shear stress-strain for stress paths which encompasses a wide range of change in shear stress ratio (e.g. CKoUE).

In order to define the stress reversal point (SRP) in the elastic realm, a scalar strain amplitude parameter, $\chi$, is introduced through the following expressions:

$$\dot{\chi}=\begin{Bmatrix} {}^{\Delta l}\varepsilon_v \delta\varepsilon_v \quad for\ \delta\varepsilon_v \neq 0 \\ {}^{\Delta l}\boldsymbol{\varepsilon}_s : \delta\boldsymbol{\varepsilon}_s \quad for\ \delta\varepsilon_v = 0 \end{Bmatrix} = \begin{cases} >0 & loading \\ \leq 0 & unloading \end{cases} \tag{5}$$

where ${}^{\Delta l}\varepsilon_v$ and ${}^{\Delta l}\boldsymbol{\varepsilon}_s$ are the volumetric and deviatoric accumulated strain with respect to the last stress reversal state ( ${}^{\Delta l}\varepsilon_v = \varepsilon_v - \varepsilon_{v,rev}$ and ${}^{\Delta l}\boldsymbol{\varepsilon}_s = \boldsymbol{\varepsilon}_s - \boldsymbol{\varepsilon}_{s,rev}$ ).

**Bounding surface plasticity.** We used the concept of bounding surface plasticity to generate plastic strain and excess pore pressure within a single yield surface as two essential elements to simulate the cyclic response. As shown in Fig. 4, plastic behavior at the current stress point anywhere within the bounding surface is linked to the plastic response of the corresponding image point on the bounding surface (i.e. corresponding to NC condition) using radial mapping. Formulation of the constitutive model in the present study introduces two mapping rules. The formulation of the mapping rule for the flow direction in multi-axial stress space is expressed as below:

$$\begin{aligned}
&\mathbf{P} = (1-g_1)\mathbf{P}^I + \mathbf{P}^o g_1 \left(\frac{p_{0,NC}}{p_0}\right)^2 && \gamma = \exp\left[\xi_v(\varepsilon^p_{acc,v} + \varepsilon^p_{acc,q})\right] \\
&P_v = (1-g_1)P_v^I + P_v^o g_1 \left(\frac{p_{0,NC}}{p_0}\right)^2 && \varepsilon^p_{acc,v} = \sum \left| d\varepsilon_v^p \right| \\
&P_v^o = -\left(\frac{3}{p_0}\right)\sqrt{\left|\mathbf{P}_s^I : \mathbf{Q}_s^I\right|(\mathbf{S}:\mathbf{S})} && \varepsilon^p_{acc,q} = \sum \left| d\varepsilon_q^p \right| = \frac{2}{3}\sum\sqrt{trace\left(d\boldsymbol{\varepsilon}_s^p : d\boldsymbol{\varepsilon}_s^p\right)} \\
&\mathbf{P}_s = \mathbf{P}_s^I \; where \; \mathbf{P}_s^o = \mathbf{0} && P_v^I = trace\left(\frac{\partial g}{\partial \boldsymbol{\sigma}}\right) = \frac{\partial g}{\partial p} \\
&g_1 = (g_1')^\gamma = \left(\frac{p_o^I - p_o}{p_o^I - p_o^i}\right)^\gamma && \mathbf{P}_s^I = \frac{\partial g}{\partial \boldsymbol{\sigma}} - \frac{1}{3} trace\left(\frac{\partial g}{\partial \boldsymbol{\sigma}}\right)\mathbf{I} = \frac{\partial g}{\partial \mathbf{S}} \\
& && \mathbf{Q}_s^I = \frac{\partial f}{\partial \boldsymbol{\sigma}} - \frac{1}{3} trace\left(\frac{\partial f}{\partial \boldsymbol{\sigma}}\right)\mathbf{I} = \frac{\partial f}{\partial \mathbf{S}}
\end{aligned} \tag{6}$$

where $P_v^o$ and $\mathbf{P}_s^o$ are the volumetric and deviatoric flow directions at first yield (i.e., first loading for stress states within the bounding surface), and $P_v^I$ and $\mathbf{P}_s^I$ are the volumetric and deviatoric flow directions at image point on the bounding surface. $g_1$ is the mapping function

which is formulated based on the size of the first or initial loading surface, $p_o^i$, current loading, $p_o$, and the bounding surface plasticity $p_o^I$. $p_{0,NC}$ is the size of bounding surface before the first unloading. $\xi_v$ is a dimensionless material constant which controls the amount of plastic strain generated at the end of each cycle. This parameter is calibrated using unload-reload path in the consolidation test through trials to obtain the best fit to match the reloading path characterized by the plastic strain. This parameter is also the key factor affecting the soil cyclic response.

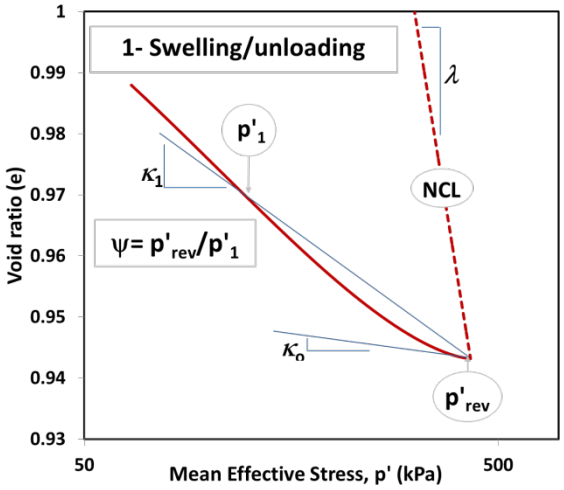


Figure 3- Definition of parameter, $\psi$, during unloading in consolidation test

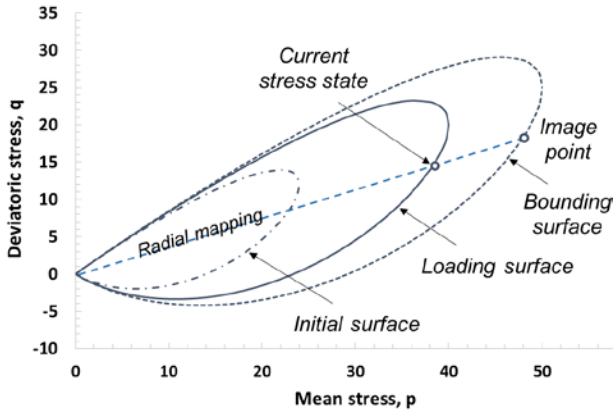


Figure 4- Schematic illustration of the lemniscate bounding surface plasticity

The mapping rule for the elastoplastic modulus is described by the following equations:

$$K_p = K_p^I + K_p^o \frac{g_1'}{(g_1'-1.0)}\left(\frac{p_o}{p_o^I}\right)^2 \left(\frac{1.5\mathbf{S}:\mathbf{S}}{\left(p_o^I\right)^2}\right)$$

$$K_p^o = \frac{p_o^I(1+e_o)}{\kappa_o}\left(1-\frac{p_o}{p_o^I}\right)\left\|\mathbf{Q}^I\right\|\left\|\mathbf{P}^I\right\|$$

$$g_1' = \left(\frac{p_o^I - p_o}{p_o^I - p_o^i}\right)$$

$$\left\|\mathbf{Q}^I\right\| = \sqrt{\left(Q_v^I\right)^2 + \frac{3}{2}\left(\mathbf{Q}_s^I : \mathbf{Q}_s^I\right)}$$

$$\left\|\mathbf{P}^I\right\| = \sqrt{\left(P_v^I\right)^2 + \frac{3}{2}\left(\mathbf{P}_s^I : \mathbf{P}_s^I\right)} \qquad (7)$$

At the first or initial yield surface right after stress reversal ( $p_o = p_o^i$), $g_1'$ function becomes equal to 1.0 and the mapping function in this equation yields to infinity ( $g_1'/(g_1'-1.0) = \infty$), which corresponds to very large elastoplastic modulus ( $K_p = \infty$), zero plastic multiplier, zero plastic strain increment, or pure elastic strain. At the image point on the bounding surface plasticity ( $p_o = p_o^I$) the mapping function becomes equal to zero, which leads to elastoplastic modulus at the image point $K_p = K_p^I$.

**Hardening:** Hardening rules, describe the evolving process of the internal or state dependent variables of the model ($p_o$, $\alpha$, $\beta$). The isotropic hardening or the evolution of $p_o$ (expansion and contraction of the yield surface) is the same as the MCC. The kinematic hardening or the evolution of $\alpha$ and $\beta$ (rotation of the plastic potential and yield surface) is also similar to SANICLAY.

**Strain rate effect:** The strain rate effect on the stress-strain-strength response of saturated clays has been extensively studied through experimental programs on wide range of clays (Kulhawy and Mayne, 1990). The rate of shearing does not have a dramatic impact on the response of OC clays, while it significantly affects the behavior of lightly over-consolidated (OCR<1.5) and NC clays (Sheahan 1991). The strain rate effect becomes more significant for high plasticity clays (Kulhawy and Mayne, 1990). Nouri (2013) and Nouri and Biscontin (2017) used the rate independent formulation calibrated by the monotonic test data and showed that the model overestimates the measured generated excess pore pressure for the cyclic response of NC clays, mainly because of not accounting for the strain rate effect. We incorporated this effect in the model parameter $m$ which controls the shape of yield surface and stress path:

$$m = 0.5 + 2\alpha_{rate}\left(\frac{p_o^I}{p_{o,NC}}\right)^2 \log\left(\frac{\dot{\varepsilon}_q}{\dot{\varepsilon}_{q,ref}}\right) \qquad (8)$$

$$\dot{\varepsilon}_q = \sqrt{trace(\dot{\boldsymbol{\varepsilon}} : \dot{\boldsymbol{\varepsilon}})} \qquad \dot{\varepsilon}_{q,ref} = \sqrt{trace(\dot{\boldsymbol{\varepsilon}}_{ref} : \dot{\boldsymbol{\varepsilon}}_{ref})}$$

$\dot{\varepsilon}_q$ state variable which is a measure of deviatoric strain rate. For shearing rates equal to the standard values (defined by $\dot{\varepsilon}_{q,ref}$) $m$ parameter reduces to constant 0.5. The typical standard shearing rate for monotonic triaxial and simple shear data in the available databases is 0.5 and 5% per hour, respectively. $\alpha_{rate}$ is a model constant which controls the rate of changes in the shape of yield surface. This parameter is calibrated by trial predictions to find the best fit for the stress path of undrained shear tests with strain rates higher or lower than the typical standard values or the stress path from the first half cycle of a cyclic test.

## MODEL EVALUATIONS

We used the experimental databases for two clays with different geotechnical characterizations to evaluate the capabilities of our constitutive formulation.

**Boston Blue Clay (BBC):** The low plasticity BBC (CL in USCS classification) is primarily composed of illite and quartz with the liquid limit of 42%, plasticity index of 19%, and about 53% of clay fraction. This moderately sensitive marine clay was deposited in the Boston Basin during the Pleistocene glaciation (Pestana, 1994). There is an extensive experimental database for BBC including monotonic and cyclic testing. Nouri and Biscontin (2017) used the database to verify the

rate independent constitutive model to predict the monotonic and cyclic clay response. Our focus in this paper is to evaluate the rate dependent formulation to capture the essential signatures of cyclic response: the generated excess pore pressure and accumulated shear strain. Table 1 summarizes the calibrated model parameters for BBC. Readers are referred to Nouri (2013) for more details on model calibration. We compared our predictions with measured data developed by Azzouz et al. (1989) through a number of undrained cyclic simple shear tests on NC and lightly OC samples of reconstituted BBC. The tests were done at the frequency of 0.1HZ with different initial shear stresses ($\tau_c$) and cyclic shear ratios ($CSR = \tau_{cyc} / \sigma_p^{'}$, where $\sigma_p^{'}$ is the maximum vertical consolidation stress). Figs. 5 and 6 compare the predictions of formulations with and without strain rate effect for normalized induced pore pressure and accumulated shear strain for NC specimens under different *CSR* with no initial shear stress. Comparison of the results indicates marked improvement in the pore pressure and shear predictions especially for the initial cycles.

**Table 1- Model parameters for BBC and GMC**

| Parameter | Description of the role | Test details | BBC | GMC |
|---|---|---|---|---|
| $\lambda$ | Compressibility of NC Clay | Consolidation test: $K_o$ or 1-D (Oedometer, $K_o$ Triaxial or *CRS* Tests) or Hydrostatic (Isotropic Triaxial) | 0.184 | 0.247 |
| $D$,<br>$n$ | Non-linear volumetric swelling and perfect hysteresis | | 25<br>1.6 | 8<br>1.6 |
| $\zeta_v$ | Irrecoverable plastic strain for unload-reload cycle | | 162 | 160 |
| $\nu$ | Elastic Poisson's Ratio | $K_o$ Oedometer or $K_o$ Triaxial | 0.26 | 0.3 |
| $K_{oNC}$<br>$x$ | $K_{oNC}$: for NC Clay<br>$x$: Saturation limit of anisotropy (for $\eta$=$q$/$p$=const.) | | 0.48<br>2.16 | 0.66<br>2.54 |
| $\kappa_o$ | Maximum elastic compressibility factor | Shear wave velocity or $G_{max}$ measurement | 0.001 | 0.007 |
| $M_c$<br>$M_e$ | Slope of critical state line triaxial comp./extension | Undrained shear compression/extension test | 1.348<br>0.932 | 0.941<br>0.765 |
| $N$ | Shape of the yield surface | Undrained shear test | 1.62 | 2.30 |
| $C$ | Rotational rate of yield surface and plastic potential | | 4.0 | 0.2 |
| $w$ | Small strain non-linearity shear | | 0.3 | 0.4 |
| $\alpha_{rate}$ | Strain rate effect | Undrained shear test with high strain rates or first half cycle of a cyclic test | 0.3 | 0.3 |

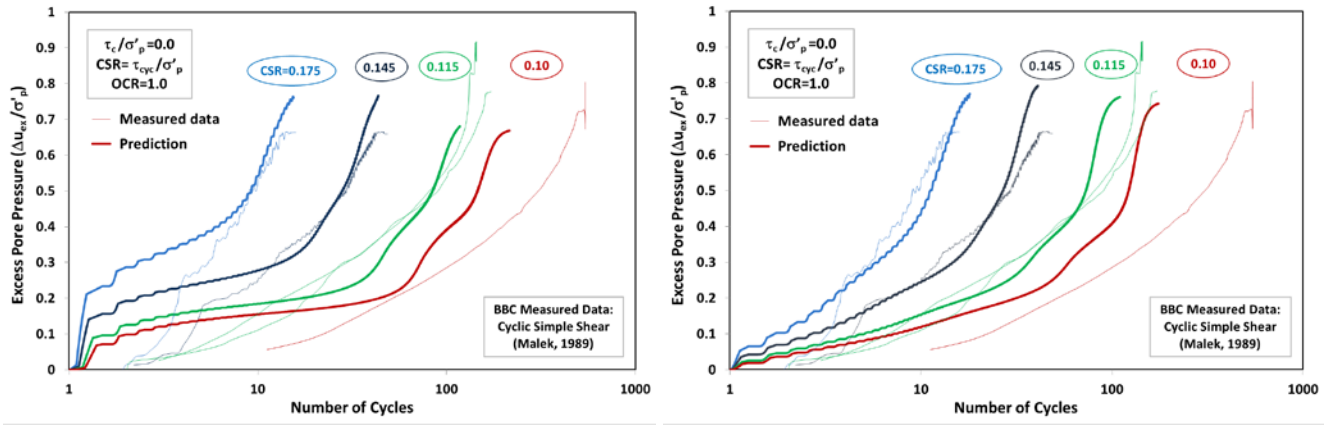


(a) (b)

Figure 5- Comparison of model predictions and measured data for excess pore pressure versus number of cycles, NC BBC with no initial shear stress: (a) without strain rate effect; (b) with strain rate effect

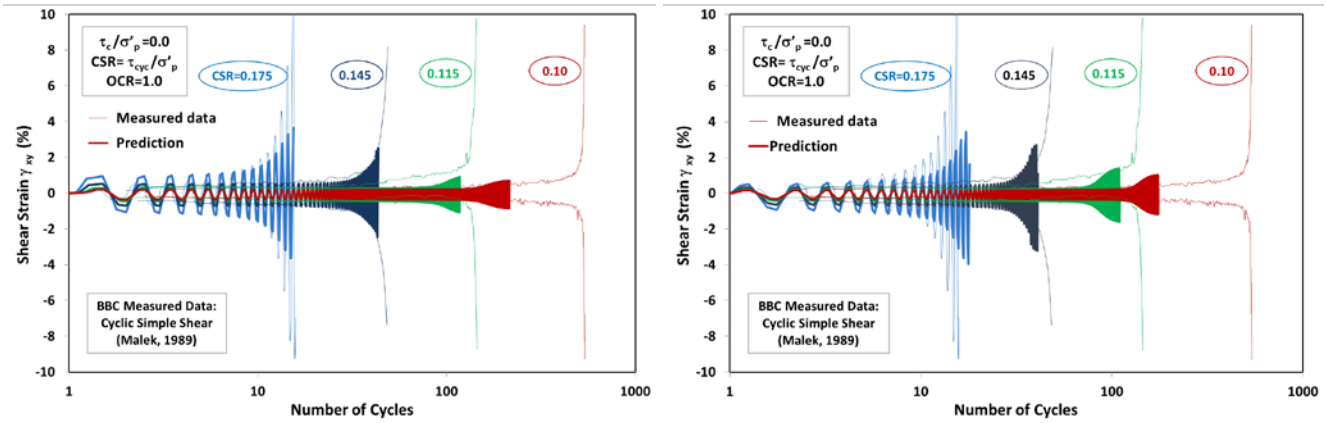


(a) (b)

Figure 6- Comparison of model predictions and measured data for accumulated shear strain versus number of cycles, NC BBC with no initial shear stress: (a) without; (b) with strain rate effect

Figure 7 shows the results of modified rate dependent formulation for NC clay samples under initial shear stress ratio of $\eta_c = \tau_c / \sigma_p^{'} = 0.1$. The initial shear stress could be representing a sloping ground of approximately 6 degrees inclination angle. As measured data indicates, a shallow sloping ground is sufficient to cause the same level of shear strain and pore pressure in much less number of cycles compared to level ground. This feature is reasonably simulated by our constitutive formulation.

**Gulf of Mexico Clay (GMC)**: Gulf of Mexico soft clay is a marine high sensitivity fat clay (CH in USCS classification), liquid limit of 60-100%, plasticity index of 40-60%, and clay fraction of about 50-70%. We also evaluated the model formulation for GMC sediments using a database developed in an effort parallel to this study, with the motivation of developing a better insight of triggering mechanisms of submarine landslides, mainly caused by cyclic seismic and wave loading. The database includes index testing, constant rate strain (CRS) consolidation, *Ko*

consolidated undrained compression and extension monotonic triaxial tests along with a series of monotonic and cyclic simple shear tests on undisturbed GMC samples at Texas A&M University (Rutherford 2012). Rutherford (2012) also conducted cyclic, circular, and figure 8 multidirectional simple shear tests. Our focus in this paper is to demonstrate the modified model capabilities to predict the mono- and multi-directional cyclic stress paths and the readers are referred to Nouri (2013) for the calibration process and evaluation of the model for monotonic shear stress paths.

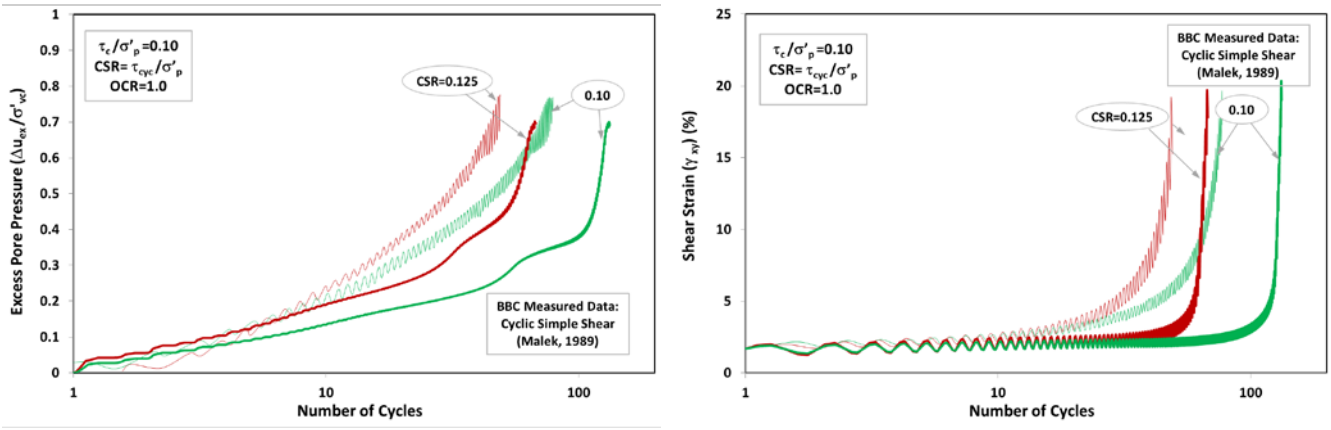


(a) (b)

Figure 7- Comparison of model predictions and measured data for NC BBC under cyclic simple shear with $\tau_c = 0.1\sigma'_p$: (a) excess pore pressure; (b) accumulated shear strain

As shown in Figure 8, the model formulation reasonably captures the generated excess pore pressure and shear strain for the NC GMC subjected to cyclic simple shear with the measured data. Figures 9 and 10 also compare the predictions of the model with and without the strain rate effect in comparison with the measured data for a circular multidirectional simple shear test on an NC GMC. Figure 9 highlights the significant improvement of excess pore pressure predictions (about 60 to 70%) in the modified formulation (i.e. with the strain rate feature) especially in the beginning cycles. The results also underscore the significance of accounting for strain rate effect in the model formulation to simulate multidirectional cyclic stress paths. Figure 10 also compares the shear strain predictions for the two formulations with and without strain rate effects with the measured data for circular stress path. Note that shear strain in multidirectional loading is defined as $\gamma = \sqrt{\gamma_x^2 + \gamma_y^2}$ where $\gamma_x$ and $\gamma_y$ are the shear strain in $x$ and $y$ directions. Generally, the model predictions of formulation with no rate effect are fairly in agreement with the measured data. Although predictions with the rate effect are improved, the incorporation of rate effect in the shape of yield surface (and not the plastic potential surface) does not have a marked impact on the shear strain predictions, which is the favorable from the constitutive formulation development perspective.

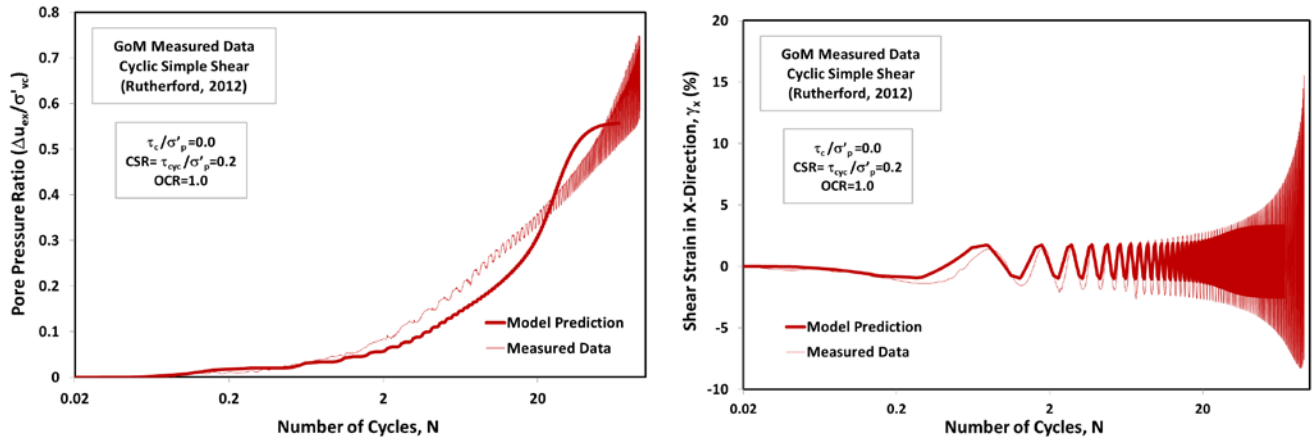


(a) (b)

Figure 8- Comparison of model predictions and measured data for NC GMC under cyclic simple shear with initial shear stress of $\tau_c = 0.2\sigma'_p$: (a) excess pore pressure; (b) accumulated shear strain

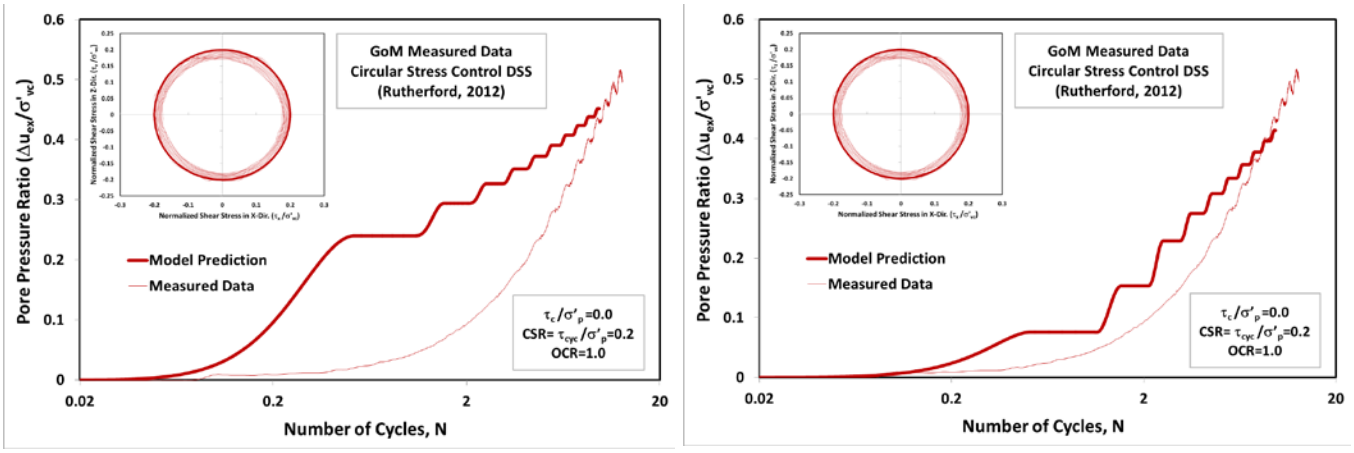


(a) (b)

Figure 9- Comparison of excess pore pressure predictions and measured data for NC GMC under circular simple shear with $\tau_c = 0.2\sigma'_p$: (a) without strain rate effect; (b) with strain rate effect

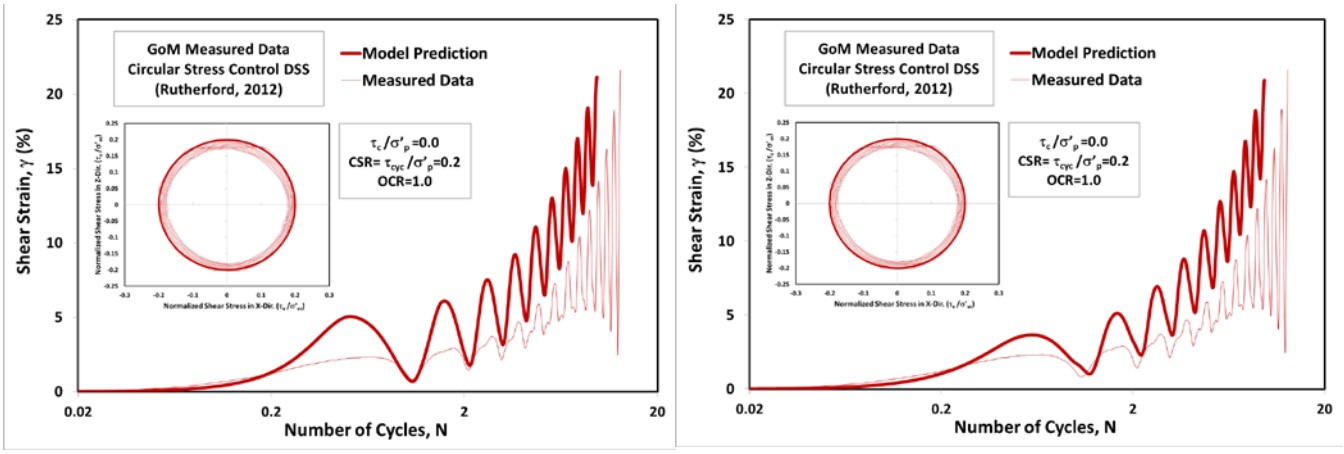


(a) (b)

Figure 10- Comparison of shear strain predictions and measured data for NC GMC under circular simple shear with $\tau_c = 0.2\sigma'_p$: (a) without strain rate effect; (b) with strain rate effect

## CONCLUSION

This paper presents the constitutive formulation, model parameters, and the predictive capabilities of a constitutive model for clays. The model is capable of predicting a wide range of monotonic shear stress paths for different clay types and OCRs. The modification in the formulation to account for strain rate effect also offers significant improvements in the model predictions and enables to reasonably capture the main signatures of complicated mono- and multi-directional cyclic stress paths.

## REFERENCES


Azzouz, A.S., Malek, A.M., and Baligh, M.M. (1989). "Cyclic behavior of clays in undrained simple shear." *Journal of Geotechnical Engineering*, 115(5), 637-657.

Beaty, M.H. and Byrne, P.M. (2011). UBCSAND constitutive model: Version 904aR. Report: UBCSAND Constitutive Model on Itasca UDM Web Site, February 2011.

Dafalias, Y.F., Manzari, M.T., and Papadimitriou, A.G. (2006). "SANICLAY: simple anisotropic clay plasticity model." Inte*rnational Journal for Numerical and Analytical Methods in Geomechanics*, 30(12), 1231-1257.

Kulhawy, F.H., and Mayne, P.W. (1990). Manual on Estimating Soil Properties for Foundation Design. Electric Power Research Institute EL-6800, Project 1493-6, Electric Power Research Institute, Palo Alto, CA.

Nouri, H. (2013). Numerical methods in offshore geotechnics: applications to submarine landslides and anchor plates. Ph.D. Thesis, Texas A&M University, College Station, TX.

Nouri, H. and Biscontin, G. (2017). "Cyclic Response of Clay Deposits: Developing a Constitutive Model." *3rd International Conference on Performance-based Design in Earthquake Geotechnical Engineering (PBD-III)*, July 2017, Vancouver, BC, Canada.

Pestana, J. (1994). A unified constitutive model for clays and sands. Ph.D. Thesis, Massachusetts Institute of Technology, Cambridge, MA.

Rutherford, C.J. (2012). Development of a multi-directional direct simple shear testing device for characterization of the cyclic shear response of marine clays. PhD Thesis, Texas A&M University, College Station, TX.

Sheahan, T.C. (1991). An experimental study of the time-dependent undrained shear behavior of resedimented clay using automated stress-path triaxial equipment. Sc.D. Thesis, Massachusetts Institute of Technology, Cambridge, MA.

Whittle, A. and Kavvadas, M. (1994). "Formulation of MIT-E3 constitutive model for ooverconsolidated clays." *Journal of Geotechnical Engineering*, 120(10), 173-198.

Ziotopoulou, K. and Boulanger R.W. (2013). "Calibration and implementation of a sand plasticity plane-strain model for earthquake engineering applications." *Journal of Soil Dynamics and Earthquake Engineering*, 53, 268-280.